

INTEGRATION OF TERRESTRIAL LASER SCANNER FOR GROUND NAVIGATION IN GPS-CHALLENGED ENVIRONMENTS

X. Wang^{a,*}, C. Toth^{a,b}, D. Grejner-Brzezinska^a, H. Sun^a

^a Satellite Positioning and Inertial Navigation (SPIN) Laboratory - (wang.1144, toth.2, brzezinska.1, sun.248)@osu.edu

^b Center for Mapping

The Ohio State University, Columbus, USA

Commission V, WG V/3

KEY WORDS: Laser scanning, Automatic registration, Feature extraction, Point cloud processing, Navigation

ABSTRACT:

GPS/INS integration can provide high accuracy (centimeter level) navigation under good satellite geometry and atmospheric conditions. However, due to GPS signal blockage and accumulative error attributes of INS, a GPS/INS system cannot continuously maintain such high accuracy navigation during GPS outages, which may frequently happen in terrestrial applications, such as when navigating in forested areas. Imaging sensors can provide adequate data to support navigation in these situations. Due to its high accuracy and efficient range measuring capabilities, we propose the integration of a terrestrial laser scanner into a navigation system, primarily for calibrating the INS. To attain centimeter level navigation accuracy in any environment under heavy canopy, spherical objects are placed around the navigation area; they remain stationary during navigation. Using a conic search window, a spherical point cloud search is performed. Then, the center positions of the spheres are determined by a least squares method. Sphere centers extracted from different scans are registered based on their topology, and the differences between the scanner's positions and attitudes at different scanning sites, the relative positioning result in a local coordinate frame, are accurately computed and subsequently used for the calibration of the INS. This paper discusses the integration of a terrestrial laser scanner into a GPS/INS/pseudolite (terrestrial RF system) integrated terrestrial navigation system, and provides preliminary simulation test results.

1. INTRODUCTION

1.1 Motivation

The integration of GPS and INS is the standard (and optimal) navigation solution for applications with good GPS availability, where high accuracy navigation (centimeter level) can be obtained under good satellite geometry and atmospheric conditions. However, this is not the case in terrestrial applications, especially in urban canyons and under dense canopy, where the GPS signal is often blocked and where the INS error will accumulate without bounds. One of these challenging applications is the detection and remediation of munitions and explosive-of-concern (MEC), in which a centimeter-level navigation solution is needed to register geophysical sensors for accurate spatial mapping of magnetic or electromagnetic signatures around suspected areas.

Due to its high accuracy (millimeter level) and efficient range measuring capabilities (hundreds of thousands points per minute), a terrestrial laser scanner is a good candidate for sensor positioning and navigation, and thus, can be integrated with other sensors to provide a precise and reliable navigation solution (Campbell *et al.*, 2006; Joerger and Pervan, 2006; Soloviev *et al.*, 2007; Vadlamani and Uijt de Haag, 2007). In an integrated system consisting of a laser scanner and GPS/INS, the laser scanner can bridge the gaps when GPS signals are blocked. In an experimental system, meter-level absolute positioning accuracy was reported for 47-second GPS outages in urban environments (Joerger and Pervan, 2006). A laser scanner can be tightly integrated with an INS, and the integrated navigation performance of the system is mainly

dependent on INS accuracy. Studies have shown that meter-level accuracy is achievable for a 200-meter trajectory (160 seconds) in a challenging urban environment with an integrated system using a tactical-grade INS and a medium level laser scanner (Soloviev *et al.*, 2007).

Surface matching, or 3D point cloud registration, is a critical aspect of using TLS sensors to support navigation. Iterative Closest Point (ICP) is one of the most popular algorithms for surface matching (Besl and McKay, 1992; Chen and Medioni, 1992). ICP was designed to search for the nearest points in two point sets, on the assumption that every point of a surface in one point set has a corresponding point on a matching surface. With good initialization, ICP is capable of producing precise transformation parameters. The Least Squares 3D Surface Matching (LS3D) method is another widely used technique (Gruen and Akca, 2005). In *ibid.*, LS3D is used to match one or more 3D search surfaces to a 3D template surface by minimizing the sum of the squares of the Euclidean distances between these surfaces. The localization and elimination of erroneous areas and areas of occlusion is possible with this method; however, good initial approximations are needed.

An integrated method for point cloud registration is found in (Rabbani *et al.*, 2007). The indirect method segments the points into certain objects and calculates the scene registration parameters by minimizing the sum of square differences of the object parameters. The direct method simultaneously calculates the registration parameters and object parameters based on the minimization of orthogonal distances of points from their surfaces. In that effort, the planes and cylinders were semi-automatically recovered.

* Corresponding author.

1.2 Principles of using TLS for navigation

The goal of the research effort described in this paper is to design, implement and test a high accuracy hybrid navigation system that can meet the stringent requirements of a man-portable geophysical mapping system, and is capable of maintaining high relative positioning accuracy in GPS-challenged environments (Grejner-Brzezinska *et al.*, 2008). This navigation system is intended to integrate Differential GPS (DGPS), INS, pseudolite (PL, terrestrial RF system), and terrestrial laser scanning (TLS) and uses an Extended Kalman Filter to integrate the information from the four sensors for an optimal hybrid navigation solution.

In our approach, the TLS is used to provide relative positions to restrict the error accumulation of INS, when the GPS and PL signals are partly or totally blocked. Since the accuracy requirements for relative positioning are very stringent (centimeter level), the establishment of a network of spherical targets in the survey area is proposed. The spherical targets are easy to identify and can be positioned with high accuracy, resulting in an improved surface matching performance, and ultimately, it translates into robust navigation performance.

Using spherical objects, the point clouds are efficiently scanned with a conic search window to find the points of spherical targets, and then a segmentation method is applied to distinguish target points from non-target points. The center positions of the spheres are determined with a least squares method. Exploiting the topology of the spheres, sphere centers in different scans are co-registered and the differences between the scanner's positions and attitudes at different scanning sites, as well as, the relative positioning results in a local coordinate frame, are accurately derived and used for INS calibration.

2. SPHERE CENTER DETERMINATION

Research on detecting spheres in laser point clouds is reported in (Ogundana *et al.*, 2007), where the Hough transformation is employed to determine sphere centers and a hash table is established to solve the data storage problem. Due to the difficulty in accurate estimation of the sphere normals with sparse points, the Hough transform method is not used here. Instead, a method has been developed, including four steps, look-up table (LUT) indexing, sphere point classification, least squares fitting, and sphere center refining.

2.1 LUT Indexing

LUT indexing establishes a direct link between a two dimensional array and laser points, where the array is indexed based on the horizontal and vertical angles of the laser points. The main advantage is that neighboring points that may be located on different scan lines can be efficiently accessed using the index table.

2.2 Sphere Point Classification

Two methods have been developed and compared for sphere point classification, namely, the smallest range variation algorithm and the region growing algorithm.

The smallest range variation algorithm searches the LUT with an adaptive search window width, and when the ranges in this

window satisfy some conditions, a least squares fitting is applied to estimate the possible "sphere" center with the selected points. As depicted in Figure 1, if a point is on the sphere, the range difference between the measured range of this point and the shortest range should meet the condition

$$\Delta s \leq \sqrt{s^2 + 2rs} - s \quad (1)$$

where s – the shortest range
 r – the radius of the spherical object

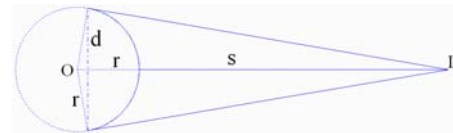


Figure 1. Relationship between the shortest range and other ranges to sphere points

This is a rather simple sphere point classification criterion, and for occluded and noisy data, a constant may be added to the right side of Equation (1) to compensate for occlusion and noise. The initial search window width can be set according to the average or largest range in a data set and the radius of spherical objects.

The region growing algorithm segments points in a search window into different groups (objects) and then tries to fit points of every group into a sphere. This algorithm is based on distances between a point and its eight neighbors indexed in the LUT. If one of them is within a pre-defined distance threshold, that cell is labeled with the same group number of the current cell. After searching all eight neighbors, the search window moves to the newly labeled cell and continues searching. If no neighbor cell is labeled for one cell, this group is closed and a new search with a new group number starts from one of the remaining unlabeled cells. When all the cells in the search window have been labeled, they will be clustered to groups. For every group, least squares fitting is used to estimate the feasible sphere center candidates.

For both algorithms, sphere center refinement is needed to allow for the inclusion of a maximum number of sphere points into the sphere center estimation process.

2.3 Least Squares Fitting

Differentiating the equation of a sphere, it can be acquired that

$$r - r_i = \frac{(x_0 - x_i)}{r_i} \delta x + \frac{(y_0 - y_i)}{r_i} \delta y + \frac{(z_0 - z_i)}{r_i} \delta z + e_i \quad (2)$$

where x_0, y_0, z_0 – the approximate sphere center
 x_i, y_i, z_i – the i^{th} measured sphere point
 r – sphere radius (known)
 r_i – distance from the i^{th} point to approximate center
 $\delta x, \delta y, \delta z$ – corrections to sphere center coordinates
 e_i – residual

The unknowns, $(\delta x, \delta y, \delta z)$, can be resolved with a least squares adjustment according to the principle

$$\tilde{e}^T P \tilde{e} \rightarrow \min \quad (3)$$

where \tilde{e} – estimates of the residuals
 P – weight matrix

The standard deviation of the least squares fitting can be estimated with

$$\hat{\sigma}_0 = \sqrt{\frac{\tilde{e}^T P \tilde{e}}{n-3}} \quad (4)$$

where n – sphere point number

It should be noted that this is an iterative process, and the initial values of the sphere center coordinates are approximated with the coordinate averages of the selected points.

2.4 Refining Sphere Centers

The sphere center refining process is designed to assure that the maximum number of correct sphere points is included into the sphere center computation. In the first step, sphere centers within a certain threshold are averaged; this situation may arise from overlapping search windows. Next, the exact search window width, D , can be determined according to the averaged sphere center as

$$D = 2d = \frac{2r\sqrt{s^2 + 2rs}}{s+r} \quad (5)$$

where the notations are identical to Equation (1).

Searching the sphere points with the resized search window, the averaged center can be used to add another condition for the sphere point classification, i.e., distances from points to this center should be less than a given threshold. During the refining process, if the candidate is a false center and the point distribution is far from a sphere surface, the refining condition may decrease the amount of selected points, and thus, leads to the automatic removal of the false candidate.

3. SPHERE CENTER MATCHING

The objective of the sphere center matching is to relate the spherical targets scanned from various positions to each other. The currently used algorithm is based on distance matching and is not yet optimized to efficiently handle larger number of targets. Primarily due to occlusion, the geometric configurations of the extracted sphere centers, measured at different scanning sites vary, yet at least a good number of line segments are identical. Based on this concept, the sphere center matching starts by finding one or two line segment pairs between two data sets for which the line segments have the same lengths, and thus, could link sphere centers to each other. Next, sphere center pairs between two data sets are determined based on having the same sum of distances to the end points of the matched line segments. Finally, the end points of the line segments can be matched with the same method, i.e., if an end point has the same sum of distances to the already matched points in a data set with that of an end point in another data set, they are assumed to be of the same spherical object.

A modification to the above described method is the introduction of clockwise (or anticlockwise) indexing of the sphere center points and comparing the lengths between consecutive points of the two data sets to find the matching line segment pairs. This solution can reduce the possibility of mismatching while simultaneously improving computation efficiency. The distances between two identical sphere centers measured at two different scan sites differ by the accuracy of the sphere center determination, and thus, an appropriate threshold is used for length comparison.

After sphere center matching, the coordinates of the sphere centers in the second or any subsequent data set, or local frame, can be transformed to the first local frame with a similarity transformation. Since the coordinates of the laser scanner can be coarsely determined by the INS, the transformation angles between two data sets are usually small, and therefore, a six or seven parameter similarity transformation is adequate. Finally, the position and orientation changes of the system platform can be derived based on resection.

4. TLS-BASED RESECTION

When a minimum number of sphere centers of two scans have been matched, the changes in position and orientation of the system platform between the two scanning locations can be derived through spatial resection (Figure 2), and subsequently used for calibrating the INS.

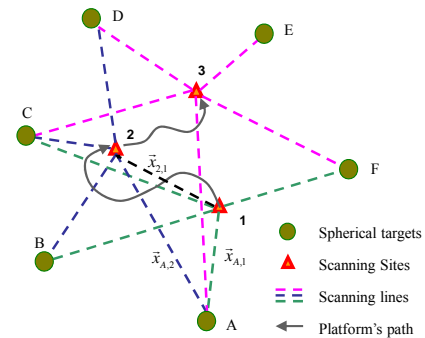


Figure 2. The spatial resection concept using TLS ranges and spherical targets

The derived position and attitude information is fed directly to the Kalman filter, as formulated by the following equation (Grejner-Brzezinska *et al.*, 2008).

$$X_1^n + R_{b1}^n X_{p,1}^{b1} - X_2^{n0} - R_{b2}^{n0} X_{p,2}^{b2} = -\delta X_2^n + X_{p,2}^{n0} \varepsilon \quad (6)$$

where

- X_1^n – coordinates of site 1 in the navigation frame
- R_{b1}^n – transformation matrix from the first local frame of TLS to navigation frame
- $X_{p,1}^{b1}$ – the first frame coordinates of the common targets observed at site 1
- X_2^{n0} – approximate coordinates of site 2 in navigation frame

- R_{b2}^{n0} – approximate transformation matrix from the second local frame of TLS to navigation frame
- $X_{P,2}^{b2}$ – the second frame coordinates of the common targets observed at site 2
- ΔX_2^n – the coordinate error vector
- $X_{P,2}^{n0}$ – the skew-symmetric matrix of the coordinate vector
- ε – the attitude angle error vector

5. SIMULATION TEST RESULTS

Various TLS data sets were simulated to test the sphere center determination and sphere center matching algorithms. In addition, to evaluate the efficiency of the integrated system, further tests were implemented by substituting the GPS signal with simulated TLS navigation results in a GPS/INS navigation system, which allowed for the comparison of the INS/TLS results with the GPS/INS reference solution.

5.1 Sphere Center Determination Result

Test results on sphere center determination with the simulated data, depicted in Figure 3, are reported in (Grejner-Brzezinska *et al.*, 2008). Both the smallest range variation algorithm and region growing algorithm could correctly derive the sphere centers from the original TLS data (without noise). For the occluded and noisy data, as shown in Figure 3, the smallest range variation algorithm could determine the true sphere centers, but false sphere centers were also fitted and difficult to remove in the refining process. With the region growing algorithm, where the minimum number of points for least squares fitting was fourteen, all sphere centers were correctly determined, and four false sphere center candidates were automatically removed in the refining process. The final results show that the derived sphere centers have accuracy better than 8.0 millimeters even when the data noise is at the one centimeter level for every coordinate component (Grejner-Brzezinska *et al.*, 2008).

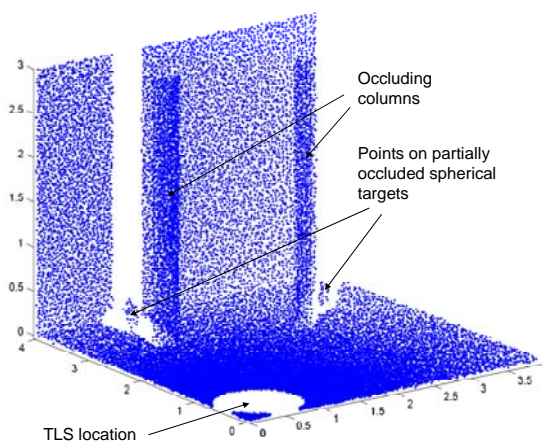


Figure 3. Simulated TLS data with occlusion and one centimetre noise

Concerning computation efficiency, the sphere center determination with the region growing algorithm takes 3-4

minutes for a data set of 80,000 points using 50 percent overlap between search windows.

5.2 Sphere Center Matching Results

In order to better test the sphere center matching algorithm, the next scenario simulated eight spherical objects with the same radius (0.20m) distributed on flat ground with an area of 30×30 square meters; a laser scanner was initially located at the lower left part of the scene, and then moved to the upper right part, see Figure 4. Moreover, two meter translations in both x and y directions, and a one degree rotation about the z-axis were added to the second local frame. The TLS data was simulated with two centimeter random noise, the scanning increment in both directions was ten arc minutes, and the distances from spherical objects to the laser scanner ranged from 3 to 28 meters.

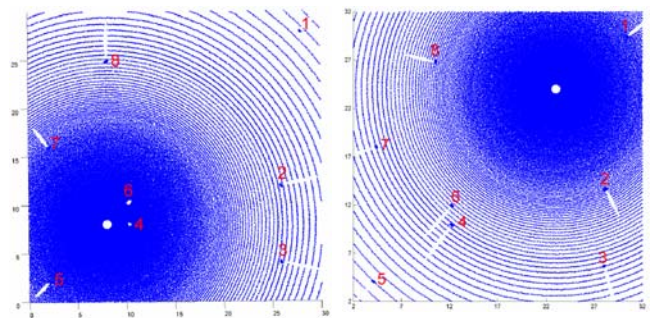


Figure 4. Eight spheres scanned at two sites

Using the region growing algorithm, with the minimum number of points setting to twelve, all the sphere centers could be uniquely determined except for sphere 1 in the first scan; sphere 1 had only seven points (Figure 4). By lowering the minimum number of points to seven or less, sphere 1 could be extracted. However, in this case, false “spheres” were also detected. The smallest range variation algorithm was also able to derive all the sphere centers in the first data set by setting the search window as small as 3×3, but it also produced false results in the small window cases. The extracted sphere centers are depicted as circles (left) for the first scan and triangles (right) for the second scan in Figure 5.

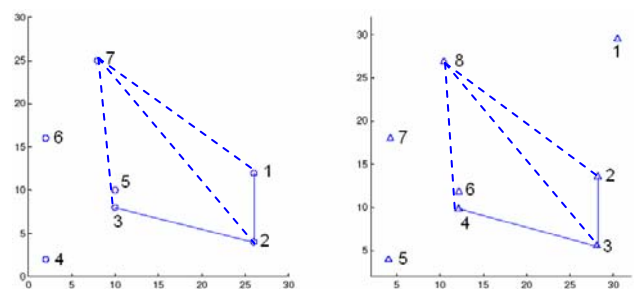


Figure 5. Derived sphere centers from two scans and the matched line segments for sphere center matching

In the sphere center matching, the single distance difference (length) threshold was set to five centimeters and the sum of the distances threshold to 50 centimeters. The matched line segments were L_{12} , L_{23} in the left, and L_{23} , L_{34} in the right (Figure 5). By comparing the sum of the distances from other points, such as point 7 in the left and point 8 in the right, to

these end points on the matched line segments (points 1, 2, 3 in the left, and points 2, 3, 4 in the right), common points of the two scans can be determined, resulting in points 4, 5, 6, and 7 finding their corresponding points as 5, 6, 7, and 8 in the right. Subsequently, the end points of the matched line segments could be matched from the already matched points with the same method. Generally, sphere center matching for small number of points is quite accurate and efficient; run time of the test without any optimization takes only a few seconds.

5.3 INS/TLS Integrated Navigation Result

The ultimate efficiency of integrating TLS into a navigation system was tested with real field GPS/INS data and simulated TLS navigation information. As shown in Figure 6, a circular track with a good GPS/INS navigation solution (upper left) was used as a reference. Seven spherical objects, denoted as white circular points in the upper right of Figure 6, were simulated and “scanned” at site A, B and C; the inside of the triangle formed by A, B and C, represented an occlusion. The simulated TLS data are listed in Table 2, in which the distances and angles with respect to the scanning sites were either simulated or computed on the basis of the simulation values.

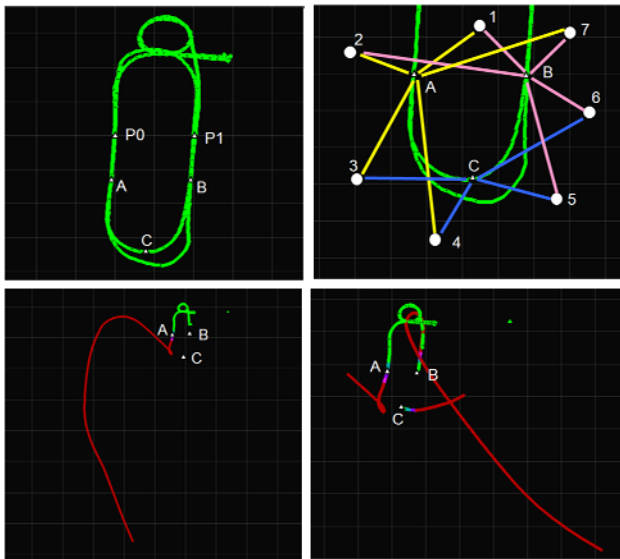


Figure 6. Simulated GPS/INS/TLS navigation solution

For the test, a GPS gap was introduced from P0 to P1, including a complete loop, and TLS data was used to calibrate INS at points A, B and C. The assumption was that the whole system moved along the former route from P0 to A and B, and after one loop back to C, then finally to P1. The time intervals (GPS gap duration) between P0, A, B, C, and P1 were 9, 35, 54, and 20 seconds respectively. With the TLS resection algorithm, the position and attitude changes relative to the first site were determined and used to calibrate the INS. The INS/TLS navigation result is depicted in the lower right part of Figure 6. As a comparison, the INS stand-alone solution is also depicted in lower left part of Figure 6. Visual interpretation suggests that at site B and C, the INS navigation solution is rectified to the correct track and keeps on the right track for a little period.

Site	Observed Sph. Obj	Distance (m)	Horizontal Angle (°)	Vertical Angle (°)	Note
A	1	7.340	220.00	2.00	Simulated
	2	6.210	105.00	4.00	Simulated
	3	11.220	30.00	-2.00	Simulated
	4	18.090	350.00	0.00	Simulated
B	7	21.850	235.00	-3.00	Simulated
	2	18.808	266.59	-6.20	Computed
	1	8.336	277.74	11.71	Computed
	7	10.112	40.87	37.36	Computed
	6	6.800	135.00	-2.00	Simulated
C	5	20.500	168.00	-1.00	Simulated
	3	14.207	202.06	-25.86	Computed
	4	7.802	223.89	-32.24	Computed
	5	11.502	22.64	34.33	Computed
	6	15.680	316.37	7.52	Computed

Table 2. Simulated TLS data in the TLS scanning frame

Quantitative comparison between GPS/INS, INS stand alone and INS/TLS navigation solutions at sites A, B, and C, as well as their relative differences to those of site A are listed in Tables 3-4. Due to the GPS gap and having no TLS calibration, the coordinate drifts at site A are -0.64 meters in east direction, -0.68 meters in north direction and 0.21 meters in up direction. The coordinates and attitude angles at sites B and C are calibrated to the same level relative to the GPS/INS solution with TLS data, and their relative accuracy with respect to site A is better than two centimeters in coordinates and 0.01 degrees in attitude. In contrast, the INS stand alone solution at site C drifts another 161 meters in position and more than 6 degrees in attitude in addition to the drifts at site A.

Unit: meter							
Site	Solution	ΔEast	Diff. to A	ΔNorth	Diff. to A	ΔHeight	Diff. to A
A	INS	-0.644	---	-0.678	---	0.208	---
B	INS	-19.552	-18.908	-21.669	-20.991	5.795	5.587
	INS/TLS	-0.660	-0.016	-0.672	0.006	0.204	-0.004
C	INS	-27.461	-26.817	-161.570	-160.892	24.885	24.667
	INS/TLS	-0.643	0.001	-0.670	0.008	0.225	-0.003

Table 3. Coordinate differences between INS/TLS, INS stand alone solutions and GPS/INS solution, and their relative differences to those of site A

Unit: degree							
Site	Solution	ΔPitch	Diff. to A	ΔRoll	Diff. to A	ΔYaw	Diff. to A
A	INS	-0.099	---	0.073	---	0.706	---
B	INS	0.086	0.185	-0.064	-0.137	1.118	0.412
	INS/TLS	-0.109	-0.010	0.071	-0.002	0.702	-0.004
C	INS	-0.396	-0.297	0.802	0.729	7.142	6.436
	INS/TLS	-0.100	-0.001	0.073	0.000	0.709	0.003

Table 4. Attitude differences between INS/TLS, INS stand alone solutions and GPS/INS solution, and their relative differences to those of site A

In spite of the achievement of high relative accuracy, the INS/TLS integrated solution brings no improvement to the absolute accuracy, as expected. It can be seen from these tables

that the absolute accuracy of the coordinates and attitudes relative to the GPS/INS solution at sites B and C are very close to that of the site A, which means TLS can effectively improve the relative position and attitude accuracy; obviously, the absolute coordinate and attitude accuracies are only dependent on the navigation accuracy of the first scan site. Another unexpected finding is that there is no apparent deficit in height accuracy compared to the horizontal accuracy in these test results, even though, theoretically, the height accuracy should be lower because of the smaller differences in height as compared to the differences in the horizontal positions of the spherical objects. This needs further investigation.

It is necessary to note that the Honeywell HG1700 (tactical grade) INS is used here, and the GPS receivers are Trimble 5700 for base station and Topcon Legacy dual frequency receiver for rover station.

6. CONCLUSION

This paper presents initial results of integration of a terrestrial laser scanner into a GPS/INS/pseudolite integrated ground navigation system for stringent application requirements. Preliminary simulation test results demonstrate that the algorithms for sphere center determination, sphere center matching, and TLS resection are quite effective and efficient. With these algorithms, the sphere points can be extracted from the TLS point cloud and the sphere centers can be determined at accuracy better than the noise level of the TLS data. The early simulation tests on system performance show that for a system integrated with a tactical grade INS, the relative positioning accuracy of the INS/TLS solution is better than two centimeters and the relative attitude accuracy is better than 0.01 degrees with respect to the first scanning site.

ACKNOWLEDGEMENTS

This research is supported by a 2007 SERDP grant.

REFERENCES

Besl, P. and N. McKay (1992). A method for registration of 3D shapes. *IEEE Transactions on Pattern Analysis and Machine Intelligence*, 14 (2), 239–256.

Campbell, J., Miller, M., Uijt de Haag, M., Venable, D., and M., Smearcheck (2006). Flash-LADAR Inertial Navigator Aiding, *IEEE/ION PLANS 2006*, April 25-27, 2006, Coronado, CA, pp. 677- 683.

Chen, Y. and G. Medioni (1992). Object modelling by registration of multiple range images. *Image and Vision Computing*, 10 (3), 145–155.

Grejner-Brzezinska, D.A., C. Toth, H. Sun, X. Wang, and C. Rizos (2008). Novel geolocation technology for geophysical sensors for detection and discrimination of unexploded ordnance, *Proceedings, IEEE/ION PLANS 2008*, May 5-8 2008, Monterey, CA, CD ROM.

Gruen, A. and D. Akca (2005). Least squares 3D surface and curve matching. *ISPRS Journal of Photogrammetry & Remote Sensing* 59 (2005) 151-174.

Joerger, M. and B. Pervan (2006). Range-Domain Integration of GPS and Laser scanner Measurements for Outdoor Navigation. *ION GNSS 19th International Technical Meeting*, September 26-29 2006, Fort Worth, TX, 1115-1123.

Ogundana, O., Coggrave, C., Burguete, R., and J. Huntley (2007). Fast Hough transform for automated detection of spheres in three-dimensional point clouds. *Optical Engineering* 46 (5) 051002.

Rabbani, T., S. Dijkman, F. van den Heuvel, and G. Vosselman (2007). An Integrated approach for modelling and global registration of point clouds. *ISPRS Journal of Photogrammetry & Remote Sensing* 61 (2007) 355-370.

Soloviev, A., D. Bates, and F. van Graas (2007). Tight Coupling of Laser Scanner and Inertial Measurements for a Fully Autonomous Relative Navigation Solution. *Proceedings of the Institute of Navigation 2006 National Technical Meeting*, 2007, San Diego, CA, 1089-1103.

Vadlamani, A. and M., Uijt de Haag. (2007). Aerial Vehicle Navigation Over Unknown Terrain Environments using Flash LADAR and Inertial Measurement. *Proceedings of ION NTM 2007*, January 22-24 2007, San Diego, CA, 1104-1118.